December 2014
Version 1.00

Scintec Flat Array Sodars

Theory Manual

SFAS, MFAS, XFAS

including RASS RAE1
and windRASS

Scintec AG
Wilhelm-Maybach-Str. 14
72108 Rottenburg
Germany

Tel [+49]-7472-98643-0
Fax [+49]-7472-9808714
E-Mail info@scintec.com
www.scintec.com

Copyright Scintec AG (2014)

Publication or distribution of this document or any part thereof only with written permission by Scintec AG, Rottenburg, Germany.

Table of Contents

1 INTRODUCTION TO SCINTEC FLAT ARRAY SODARS 1

1.1 General Features at a Glance 1

1.2 Basic Operation Principles 2

1.3 Multi-Frequency Operation 2

1.4 Multi-Beam Operation 3

1.5 Shading Mode 3

1.6 Variable Pulse Lengths 3

1.7 Maximum Height and Output Interval 4

2 SODAR THEORY 5

2.1 Velocity of Sound 5

2.2 Signal Scattering 5

2.3 Pulse Length versus Vertical Resolution 6

2.3.1 Pulse length 6

2.3.2 Frequency resolution 6

2.4 Doppler Composite 7

2.5 Wind Calculation 7

2.5.1 Doppler shift 7

2.5.2 3D-wind profiles 7

2.5.3 Standard deviations of u, v and w 8

2.6 Derived Data 9

2.6.1 Assimilated data 9

2.6.2 Wind shear 9

2.6.3 Turbulent kinetic energy 9

2.6.4 Eddy dissipation rate 10

2.6.5 Turbulence intensity 10

2.7 Non-Profile Data 10

2.7.1 Mixing height 10

2.7.2 PG-stability class 11

2.7.3 Kinematic Heat flux 11

2.7.4 Mean potential temperature 11

2.7.5 Monin-Obukov length 12

2.7.6 Friction velocity 12

3 RASS THEORY 13

3.1 Velocity of Sound 13

3.2 Temperature 14

4 WINDRASS THEORY 16

4.1 Horizontal Wind 17

5 ATMOSPHERIC EFFECTS ON SYSTEM PERFORMANCE....18
5.1 Temperature and Humidity....18
5.2 Turbulence....18
5.3 High Wind Speeds....18
5.4 Ground Clutter....18

6 REFERENCES....19

1 INTRODUCTION TO SCINTEC FLAT ARRAY SODARS

1.1 General Features at a Glance

Scintec Flat Array Sodars* are advanced and very powerful acoustic instruments for remote measurements of profiles of the three-dimensional wind speed and direction and turbulence characteristics in the lower atmosphere. There are three different models available: The XFAS is optimized for long ranges while the MFAS compromises high spatial resolution and easy portability. The SFAS is the smallest Sodar commercially available today with a high resolution of 5 m.

With their superior performance, flexibility and ease-of-operation, Scintec Flat Array Sodars not only meet the needs of routine boundary layer monitoring, but they are particularly powerful tools for a variety of research applications. Some design features of the Scintec Flat Array Sodars are:

- Acoustic antenna in flat array design with unmatched high efficiency
- 64 piezo-electric transducers (SFAS, MFAS) or 52 electromagnetic pressure chamber transducers (XFAS) for acoustic emission and reception
- Digitally-controlled phased array
- Operation with up to 10 frequencies within one pulse sequence cycle
- Beams can be emitted in up to nine directions
- Antenna can be operated in shaded or non-shaded mode for optimum side lobe suppression
- Variable pulse lengths within a single emitted sequence
- Simultaneous emission of up to 10 frequencies
- Simultaneous reception of all frequencies
- Simultaneous reception of opposite beams
- Fast Fourier Transform performed in real time
- Thickness of resolved layers down to 5m (SFAS), 10 m (MFAS) or 20 m (XFAS)
- Up to 100 (SFAS / MFAS) or 256 (XFAS) vertical layers
- Operation parameters set via auto-configuration or individually configurable by the user:
  - Number of frequencies, values of frequencies
  - Lengths of all pulses within emitted sequence
  - Number and order of used beam directions
- Real time tabulated and graphical output including
  - Horizontal wind speed and direction
  - Vertical wind speed and direction
  - Standard deviation of all wind velocity components
  - Reflectivity, temperature structure parameter C_T^2
  - Pasquill-Gifford stability classes
- All raw spectra accessible for research applications
- Automatic fixed echo detection and correction
- Low power consumption allowing battery operation (SFAS / MFAS)
- Easy interfacing with terminal PC via serial port (RS232 or RS485)
- Optional remote control via LAN, Radio or GSM Modem
- Extensive self-test capability
- Small size and light weight (SFAS / MFAS)
- Epoxy-coated aluminium body for durability even in harsh environmental conditions

* Patented, SODAR = Sound Detection and Ranging

1.2 Basic Operation Principles

Scintec Flat Array Sodars are advanced and powerful acoustic instruments for remote measurements of three-dimensional profiles of the wind speed and direction as well as turbulence characteristics in the lower atmosphere.

In operation, the antenna emits short sound pulses, which are backscattered at temperature inhomogeneities in the air. The antenna then receives the echoed sound pulses, and the amplitude and frequency of the backscattered waves are evaluated. The Scintec Flat Array Sodars are acoustic instruments of the monostatic type, i.e. the same antenna is used for emission and reception of sound.

The Scintec Flat Array Sodars generate different beam angles during emission and reception by phase delayed driving and sensing, respectively, of the rows or columns of an array of acoustic transducers. The phase delays in the emission and reception modes are produced digitally, resulting in long-term stability of the phase-shift and related performance. General advantages of phased array systems over three component horn antenna systems are smaller antenna size and more flexible use.

The height resolution is gathered by range gating, i.e. by considering the time the pulse needs to propagate from the antenna to the measured layer and back to the antenna. From the amplitude of the backscattered wave, detailed information about the turbulence structure in the atmospheric boundary layer can be obtained. By evaluating the spectrum of the backscattered wave, the wind speed is determined. This is possible because of the Doppler frequency shift resulting from the movement of the scattering temperature inhomogeneities with the mean wind. When at least three beams are emitted at different angles, a vertical profile of the three dimensional wind vector can be derived.

With the Scintec Flat Array Sodars, the spectra are determined by applying a Fast Fourier Transform to the acoustic signals received from the different directions.

The optional RASS* extension enables the system to determine temperature profiles by combining acoustic sound emission with radio wave measurements.

The optional windRASS extension enhances the RASS extension by adding the ability to perform not only temperature measurements but also wind measurements with the combined radio-acoustic measurement technique.

1.3 Multi-Frequency Operation

Scintec Flat Array Sodars can be operated in single-frequency or multi-frequency mode. In the single-frequency mode, a single pulse with a well-defined frequency is emitted and its backscattered signal is recorded and evaluated. This procedure is repeated in several directions.

In the multi-frequency mode, sequences composed of pulses of different frequencies are emitted and the backscattered waves of all frequencies are received simultaneously. Up to 10 out of 64 equally spaced frequencies in the ranges of 2540 to 4850 Hz (SFAS), 1650 to 2750 Hz (MFAS) or 830 to 1370 Hz (XFAS) can be selected. Multi-frequency operation significantly increases the signal-to-noise ratio, since more acoustic power can be emitted into the atmosphere without increasing the pulse length per frequency, i.e., without reducing the vertical resolution. As before, this procedure is repeated in several directions.

* RASS = Radio Acoustic Sounding System

1.4 Multi-Beam Operation

Scintec Flat Array Sodars can emit sonic beams in 9 different directions:

	Beam Directions SFAS		Beam Directions MFAS/XFAS	
Identifier	**Main Beam**	**Mirrored Beam**	**Main Beam**	**Mirrored Beam**
Vertical	0°	N/A	0°	N/A
North	24° North	19° South	29° North	22° South
East	24° East	19° West	29° East	22° West
South	24° South	19° North	29° South	22° North
West	24° West	19° East	29° West	22° East

Complementary pulse pairs with opposite directions (24°-19° or 29°-22°) can be emitted even within a single pulse sequence. The waves backscattered from these two directions are received simultaneously. This results in another significant increase of the signal-to-noise ratio without sacrificing vertical resolution.

Due to the unique phase delay generation technique of Scintec Flat Array Sodars, the emission angles are independent of frequency.

1.5 Shading Mode

The acoustic antenna can be operated in two modes: non-shaded and shaded mode. In non-shaded mode, the directivity of the main lobe (emission in the main direction) of the antenna is highest. In shaded mode the side lobes (emission in other than the main direction) are smallest, but in exchange, the main lobe widens slightly. For most sites the shaded mode will provide better results since it makes the measurement less sensitive to environmental noise and unwanted fixed-echo distortions. By default shading is enabled, but you can change the mode using a simple software switch.

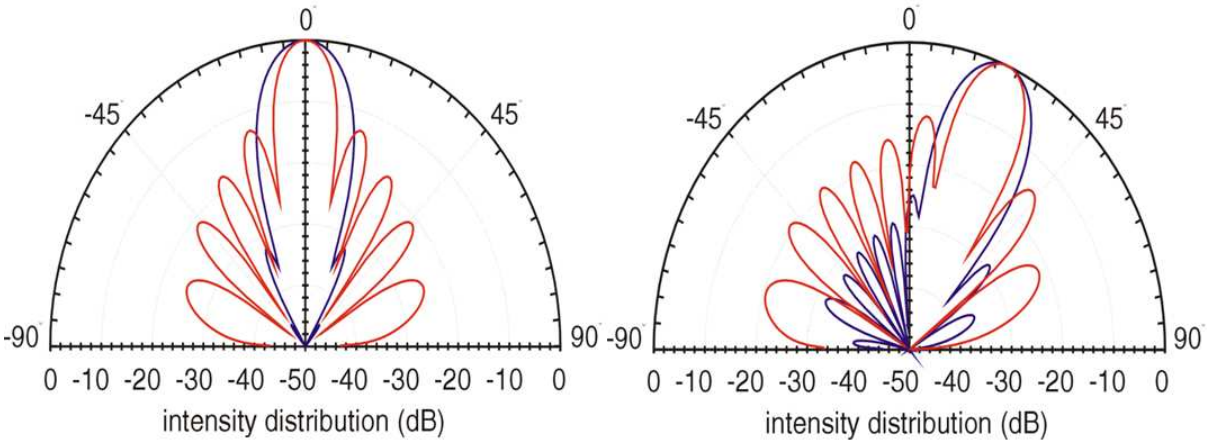

Figure 1: Beam pattern without shading (red) and with shading (blue) for the vertical (left) and horizontal beam direction (right)

1.6 Variable Pulse Lengths

Within a single emitted sequence, pulses of different frequencies or direction can have different lengths. The shortest possible pulse length corresponds to a layer thickness of 5 m (SFAS), 10 m (MFAS) or 20 m (XFAS) during data evaluation. Longer pulses are a multiple of this base length.

When multiple pulses are emitted in one sequence, the first pulses of the sequence are used to sense at higher altitudes. With the Scintec Flat Array Sodars, the lengths of the pulses

within a single sequence can vary. In particular, it is often advantageous to have a long first pulse in a sequence for a better signal-to-noise ratio at high altitudes. This increases the achievable range without sacrificing vertical resolution at lower altitudes.

Scintec Flat Array Sodars give the user full flexibility in defining the composition of the pulse sequence. The correct height referencing is automatically ensured by the evaluation software.

1.7 Maximum Height and Output Interval

The choice of the maximum measurement height is directly related to the amount of measurement time for each level. It is important to keep the maximum measurement height as low as possible. This way the amount of measurement time that will be used for each height level (i.e. the pulse repetition frequency) will be maximized and thus the data quality and availability increased. Higher maximum measurement heights require longer averaging time intervals to maintain the same data quality.

2 SODAR THEORY

The Scintec Flat Array Sodar is a remote sensing instrument. Remote sensing is often used to measure regions where it is hard to install *in-situ* instrumentation to measure directly.
The sodar provides remote measurements that are made of a volume of air some distance away from the antenna. These measurements are made by sending sound pulses in the vertical and several tilted directions. The signal is scattered back at turbulence in the atmosphere at all heights and received at the sodar antenna.
To calculate the final atmospheric properties (profiles of wind speed, wind direction, turbulence intensity, etc.), some assumptions have to be made about, for example, how sound travels through the atmosphere.

In the following, basic theoretical relations of the sodar theory and the used algorithms are briefly explained.

2.1 Velocity of Sound

The speakers create small pressure fluctuations that propagate away from the antenna. These sound waves travel through the atmosphere with the speed of sound, *c*.
The speed of sound in air is defined as the propagation velocity of the phases of acoustic waves relative to the air. Since there is no dispersion with acoustic waves, the speed of sound equals the propagation velocity of sound groups relative to the air. In the atmosphere, it equals the speed of sound in dry air with good approximation:

$$c = \sqrt{\frac{c_p}{c_v} R_g T_0} \qquad \textbf{(1)}$$

where $c_p = 1004$ J kg^{-1} K^{-1} is the specific heat of dry air at constant pressure, $c_v = 717$ J kg^{-1} K^{-1} is the specific heat of dry air at constant volume, $R_g = 287.04$ J kg^{-1} K^{-1} is the gas constant of dry air and *T* is the temperature in Kelvin. Values for the speed of sound at different air temperatures are listed in the following table:

T [°C]	*T* [°F]	*T* [K]	*c* [m/s]
-20	-4	253.15	319.0
-10	14	263.15	325.2
0	32	273.15	331.3
10	50	283.15	337.4
20	68	293.15	343.3
30	86	303.15	349.1

2.2 Signal Scattering

In the atmosphere, sound waves are scattered at turbulent temperature and wind inhomogeneities. A sodar system is called monostatic when transmitter and receiver positions are identical. This means that only direct backscatter, i.e. scattering at an angle of 180 degrees, is measured. Then wind fluctuations do not contribute to the scattering and the scattering cross section per unit volume η simply is

$$\eta = 0.0039 k^{1/3} \left(\frac{C_T^2}{T^2} \right) \qquad \textbf{(2)}$$

where k is the acoustic wavenumber

$$k = 2\pi / \lambda \quad \textbf{(3)}$$

and C_T^2 is the temperature structure function constant.

Backscatter is effective only for turbulent eddy sizes fulfilling the Bragg condition, i.e. where the spatial wavenumber of the turbulent temperature fluctuations k equals $2k$. For the validity of (3) it is required that these eddy sizes are within the inertial subrange of turbulence. For sound waves with wavelengths of the order of 0.1 m, this is usually the case.

Besides turbulent temperature structures, sound may also be backscattered at quasi-static density discontinuities. In the atmosphere, such discontinuities are formed by strong temperature inversions. Finally, particles like rain drops, snowflakes, larger cloud droplets and birds can produce backscatter.

2.3 Pulse Length versus Vertical Resolution

2.3.1 Pulse length

A sound pulse of duration t_p produces a wave group of length

$$L_p = c \cdot t_p \quad \textbf{(4)}$$

propagating through the atmosphere with speed c. After a time t_a from the end of the pulse emission, the spatial separation between the beginning and the end of the group remains

$$c(t_p + t_a) - ct_a = L_p \quad \textbf{(5)}$$

However, due to the additional time the sound needs to return to the receiver, the backscattered signal received at the emitter position after the time t_a originates from the range

$$c(t_p + t_a)/2 \quad \text{to} \quad ct_a/2 \quad \textbf{(6)}$$

The length of this group is

$$c(t_p + t_a)/2 - ct_a/2 = L_p/2 \quad \textbf{(7)}$$

In other words, it is only half as long as the actual pulse length L_p. This is called the "effective pulse length" L_e. This effective pulse length defines the achievable vertical resolution of a sodar. In other words, the achievable spatial resolution is half the length of the actual sound pulse.

2.3.2 Frequency resolution

If we consider an averaging period t_{avg}, this corresponds to a smallest resolvable vertical layer of

$$\Delta Z = t_{avg} \cdot c/2 \quad \textbf{(8)}$$

As can be shown by Fourier transform theory, the best frequency resolution achievable over a period t_{avg} is

$$\Delta f = 1/t_{av} \quad \textbf{(9)}$$

Thus, there is a principal relation between the vertical resolution of a sodar and the maximum possible frequency resolution:

$$\Delta Z \Delta f = \frac{c}{2} \quad \textbf{(10)}$$

Hence with a vertical resolution of 10 m, a frequency resolution of about 17 Hz is possible. With a frequency of 2400 Hz for example, this corresponds to a possible resolution of the vertical wind Δw of 1.2 m/s and, with $\theta = 29°$, a possible resolution of the horizontal win d ΔU

of 2.5 m/s. Due to the smooth statistics of the fluctuations of the vertical and horizontal wind components however, interpolations between adjacent frequency points finally lead to much better resolutions for the mean wind. To some degree this is valid also for the standard deviations of the wind components.

2.4 Doppler Composite

The sodar receives a backscatter profile for every pulse sequence. In multi-frequency mode typically 10 frequencies are transmitted. For every beam direction this pulse sequence is repeated *n* times (*n* = pulse repetition sequence). The backscatter signals (time series) are transformed to frequency spectra using fast Fourier transformation (FFT) for every height gate, *z*. These *n* x *z* spectra are averaged in time and used to calculate one Doppler image for each direction and each frequency. As the Doppler-shift scales with the transmitted frequency, one image is determined per frequency. A Doppler image is a 2-D image that yields information on the Doppler-shift against height.
These Doppler images are then averaged over the averaging interval which results in one Doppler image per beam direction and frequency. In case of 5 directions and 10 frequencies, 50 Doppler images are calculated.
These 50 Doppler images are finally used to calculate the composite Doppler images for all three components for the selected averaging interval. These Doppler composites are used to calculate the 3-D wind vector.

2.5 Wind Calculation

2.5.1 Doppler shift

The frequency of the backscattered signal is shifted due to the wind velocity component in the direction of the emitted sound pulse u_r. The magnitude of the frequency shift is

$$\Delta f = -2\frac{u_r}{c} f \qquad \textbf{(11)}$$

$$\Delta f_V = -2\frac{w}{c} f_V \qquad \textbf{(12)}$$

Here, f is the frequency of the emitted sound pulse. For the vertical beam with frequency f_v and the vertical wind speed w, this means in particular that δf_v is proportional to w.

2.5.2 3D-wind profiles

If we consider a beam with frequency f_E that is tilted from the vertical by an angle θ_E into eastern direction and u is the horizontal wind component in the eastern direction, the frequency shift is

$$\Delta f_E = -2\frac{u}{c} f_E \sin(\theta_E) - 2\frac{w}{c} f_E \cos(\theta_E) \qquad \textbf{(13)}$$

From this we can derive the case where 3 beams are used: one of frequency f_E which is tilted from the vertical by an angle θ_E into eastern direction, one of frequency f_N which is tilted from the vertical by an angle θ_N into northern direction and a vertical beam with frequency f_v. If we assume the three-dimensional wind to be equal in each beam at the respective layers, the easterly wind speed u, the northerly wind speed v and the vertical wind speed w are calculated from the frequency shifts via

$$u = -\frac{\Delta f_E}{2 f_E}\frac{c}{\sin(\theta_E)} + \frac{\Delta f_V}{2 f_V}\frac{c}{\tan(\theta_E)} \quad \textbf{(14)}$$

$$v = -\frac{\Delta f_N}{2 f_N}\frac{c}{\sin(\theta_N)} + \frac{\Delta f_V}{2 f_V}\frac{c}{\tan(\theta_N)} \quad \textbf{(15)}$$

$$w = -\frac{\Delta f_V}{2 f_V} c \quad \textbf{(16)}$$

Of course, f_E, f_N and f_v can be identical.

When 5 directions with the tilted angles θ_E, θ_N, θ_W, θ_S are used with the frequencies f_E, f_N, f_W, f_S respectively, and the frequency f_v for the vertical, and we assume again that the three-dimensional wind is equal in each beam at the respective layers, then we can average over the Doppler shift at opposite beams. If $\theta_E = -\theta_W$ and $\theta_N = -\theta_S$, then the contributions of the vertical wind vanish. We then simply find:

$$u = -\frac{1}{2}\left[\frac{\Delta f_E}{2 f_E}\frac{c}{\sin(\theta_E)} + \frac{\Delta f_W}{2 f_W}\frac{c}{\sin(\theta_W)}\right] \quad \textbf{(17)}$$

$$v = -\frac{1}{2}\left[\frac{\Delta f_N}{2 f_N}\frac{c}{\sin(\theta_N)} + \frac{\Delta f_S}{2 f_S}\frac{c}{\sin(\theta_S)}\right] \quad \textbf{(18)}$$

$$w = -\frac{\Delta f_V}{2 f_V} c \quad \textbf{(19)}$$

The horizontal wind direction is then calculated from *u* and *v*,

$$\phi_{wind} = \arctan(u, v) \quad \textbf{(20)}$$

2.5.3 Standard deviations of u, v and w

For every Doppler image (for every direction and every frequency) the wind components are determined. These wind components are used to calculate the standard deviations over a certain time period or number of data points *N*

$$\sigma_x^2 = \frac{1}{N-1}\sum\left(\frac{x - \bar{x}}{N}\right)^2 \quad \textbf{(21)}$$

where *x* is the wind components *u, v* or *w* and over bar indicates the mean value.

The standard deviation of the vertical wind σ_w is determined from the wind measured in the vertical direction. This means, that σ_w can be determined directly without any beam corrections.
The standard deviation of the horizontal wind components (u, v) are determined from the wind measurements in the North, East, South, West, beam direction. As these beams are not directed horizontally, these standard deviations have to be corrected.
The standard deviations of *u* and *v* are determined under the assumption that there is no correlation between σ_w and σ_u or σ_v (e.g. Bradley, 2008),

$$\sigma_u = \left[\frac{\sigma_u{}'^2}{\sin(\phi)^2} - \frac{\sigma_w{}'^2}{\tan(\phi)^2} \right]^{1/2}, \quad \textbf{(22)}$$

Where σ_u' is the standard deviation in beam direction and ϕ the beam angle. The above equation is also valid for σ_v (exchange *u* with *v*).

2.6 Derived Data

2.6.1 Assimilated data

As an input for the derived data variables, often the assimilated variables are used. The assimilated variables represent the measured data profiles fitted in time and height. This results in more robust profiles that exhibit less data outliers and data gaps.

A 2-dimensional least squares polynomial fit is used to fit the measured profiles. The time period (default is 120 min), the polynomial degree of height (default is 4) and the polynomial degree of time (default is 2) can be changed in the operational software. A weighting function which is linear from 0.25 to 1.0 over the assimilation period is used. This means that the 'newest' data weights more.

2.6.2 Wind shear

The wind shear τ in [s^{-1}] at height *z* is calculated linear from the *u*- and *v*-wind components at height z_a (one height level above) and at height z_b (one height level below),

$$\begin{aligned} \tau_u(z) &= \frac{u_a - u_b}{z_a - z_b} \\ \tau_u(z) &= \frac{v_a - v_b}{z_a - z_b} \\ \tau_{wind}(z) &= \sqrt{\tau_u{}^2 + \tau_v{}^2} \end{aligned} \quad \textbf{(23)}$$

The wind shear direction in degree is calculated from the wind shear in u and v direction,

$$\tau_{dir} = \arctan\left(\frac{\tau_v}{\tau_u} \right) \quad \textbf{(24)}$$

The assimilated wind data is used to calculate the wind shear and wind shear direction, to obtain more robust and steady profiles.

2.6.3 Turbulent kinetic energy

The turbulent kinetic energy in [m^2 s^{-2}], TKE, is estimated from the standard deviation of the vertical wind,

$$TKE = \frac{3}{2}\sigma_w^2 \quad \textbf{(25)}$$

2.6.4 Eddy dissipation rate

The estimate of the eddy dissipation rate ε [m^2 s^{-3}] is restricted to neutral or near-neutral stratification and assumes that the mechanical production of turbulence is locally balanced by dissipation (Kramar, 2001),

$$\varepsilon = TKE \cdot \frac{\tau_{wind}}{C_{KP}^{\ 2}} \tag{26}$$

The constant C_{KP} = 2.1 and is estimated from measurement data according to Kouznetsov (2000).

2.6.5 Turbulence intensity

The turbulence intensity I_{turb} is calculated using the horizontal wind speed U_{hor} and the standard deviation of the longitudinal wind speed σ_{lon} (in the direction of the wind),

$$I_{turb} = \frac{\sigma_{lon}}{U_{hor}} \tag{27}$$

To calculate the standard deviation of the wind speed in longitudinal direction σ_{lon}, it is assumed that the variance of the wind speed in the measured direction is a factor 4/3 higher than the variance of the wind speed perpendicular to the wind direction. The following weighting factors for *u* and *v* are used,

$$\begin{aligned} w_1 &= \frac{1}{2} \cdot \left[1 - \cos\left(2 \cdot \phi_{wind}\right)\right] \\ w_2 &= \frac{1}{2} \cdot \left[1 + \cos\left(2 \cdot \phi_{wind}\right)\right] \end{aligned} \tag{28}$$

The standard deviation of the wind speed in longitudinal direction is calculated,

$$\sigma_{lon} = C \cdot \left(w_1 \cdot \sigma_u + w_2 \cdot \sigma_v\right), \tag{29}$$

with using a correction factor C for the longitudinal wind speed,

$$\begin{aligned} C &= 1 + \alpha \cdot \sin\left(2 \cdot \phi_{wind}\right)^2 \\ \alpha &= \frac{\sqrt{4/3} - 1}{\sqrt{4/3} + 1} \end{aligned} \tag{30}$$

The assimilated wind data is used to calculate I_{turb}, to obtain more robust and steady profiles.

2.7 Non-Profile Data

2.7.1 Mixing height

The profiles of temperature and backscatter are used to estimate the mixing height, z_i.
The following variables are checked in the given priority order:

1. Find the lowest temperature-inversion height.
2. Find the lowest backscatter-inversion height (using the backscatter flags).
3. Or, if position 1 and 2 cannot be found, maximum backscatter and temperature range.

2.7.2 PG-stability class

The Pasquill-Gifford stability class is calculated according the $\sigma\phi$– method (EPA, 2000), which is based on the standard deviation of the elevation angle of the wind ($\sigma\phi$). The roughness length z_0 is set to 0.15 m (standard value) and can be changed in the 'advanced modelling settings' in the APRun software.

Table 1: $\sigma\phi$ boundaries valid for z = 10 m and z0 = 0.15 m

P-G stability class	$\sigma\phi$ [deg] lower boundary	Height exponent, P
A	11.5	0.02
B	10	0.04
C	7.8	0.01
D	5.0	-0.14
E	2.4	-0.31
F	0	n/a

These boundaries are valid for a measurement height of z = 10 m and a roughness length of z_0 = 0.15 m. The P-G stability class is estimated for any height and any roughness length with the following correction for $\sigma\phi$:

$$\sigma\phi_{corr} = \sigma\phi \cdot \left(\frac{z}{10}\right)^{P} \cdot \left(\frac{z_0}{0.15}\right)^{0.2} \quad . \tag{31}$$

2.7.3 Kinematic Heat flux

The kinematic heat flux is calculated only for convective conditions, which means, for PG-stability classes A, B or C.
The kinematic surface heat flux Q_0, according to Melas et al., 2000,

$$Q_0 = b^{-3/2} \cdot \left(\frac{g}{\theta}\right)^{-1} \cdot \langle w' \rangle^{3/2} \cdot z_i^{-1} \quad . \tag{32}$$

with θ as the mean potential temperature (see next paragraph) given as a fixed value (from the Hardware, Site and Environment settings) or calculated from the RASS temperature profile. And with the variance of the vertical wind w', the brackets <> indicate an average calculated over a height interval of $0.1z_i$ – $0.7z_i$.
The value b = 0.45 is a constant given by Melas et al., 2000.

The surface heat flux H_0 in [W/m²] is then calculated,

$$H_0 = Q_0 \cdot \rho \cdot c_p \quad . \tag{33}$$

With the air density ρ = 1.21 [kg/m³] and the specific heat capacity at constant pressure c_p = 1005 [J/kg/K].

2.7.4 Mean potential temperature

The potential temperature θ is calculated from the temperature T using the pressure P,

$$P = \left(1 - \frac{z}{288.15} \cdot 0.0065\right)^{5.255} \cdot 1013.25 \quad , \tag{34}$$

where z is the height of the antenna above sea level z_{asl} + the height of the antenna above ground level z_{agl} (from the Hardware, Site and Environment settings),

$$z = z_{asl} + z_{agl} \quad . \tag{35}$$

The height above sea level is calculated by the given pressure (as set in the environment settings),

$$z_{asl} = \frac{288.15}{0.0065} \cdot \left[1 - \left(\frac{P}{1013.25} \right)^{\frac{1}{5.255}} \right] \quad . \tag{36}$$

Finally the potential temperature is,

$$\theta = (T + 273.15) \cdot \left(\frac{1000}{P} \right)^{\frac{R_d}{c_p}} \quad , \tag{37}$$

with the specific gas constant for dry air R_d = 287 [J/kg/K].

2.7.5 Monin-Obukov length

The Monin-Obukov length λ is calculated iterative for convective conditions (Melas et al., 2000) using the following equations:

$$\lambda = -\frac{{u_*}^3 \cdot \theta}{g \cdot \kappa \cdot Q_0} \quad , \tag{38}$$

$$u_*(a) = \kappa \cdot \langle U \rangle \cdot \left[\ln\left(\frac{z_i}{z_0} \right) - 0.5 \cdot \ln\left(\frac{z_i}{|\lambda|} \right) - 2.3 \right]^{-1} \quad , \tag{39}$$

$$u_*(b) = \left(-\lambda \cdot g \cdot \kappa \cdot Q_0 / \theta \right)^{1/3} \quad , \tag{40}$$

with g = 9.81 m/s² the acceleration due to gravity, κ = 0.4 the von Karman constant and the mean horizontal wind <*U*>.
The solution is found for λ when [u_* (a) - u_* (b)] smallest.

2.7.6 Friction velocity

When the Monin-Obukov length λ is known, the friction velocity for convective conditions is calculated,

$$u_* = \left(-\lambda \cdot g \cdot \kappa \cdot Q_0 / \theta \right)^{1/3} \quad . \tag{41}$$

3 RASS Theory

The Radio Acoustic Sounding System (RASS) extension to Scintec's sodar instruments determines virtual temperature profiles in the atmospheric boundary layer with high spatial and temporal resolution. The RASS extension is an option that may be added to any of the Scintec Flat Array Sodars (see Figure 2). Its measurement principle rests on the detection of electromagnetic waves scattered at the known density pattern of an acoustic wave. The sodar is used to generate a vertically propagating acoustic wave, whereas the RASS transmitter generates a continuous electromagnetic wave which is detected by the receiver component in the RASS Transceiver. The electromagnetic signal is reflected at the sodar acoustic signal which travels with the speed of sound. The propagation of the speed of sound depends on the temperature and humidity of the air.

For further signal processing, the capabilities of the sodar system are employed. The setup and operation mode classify the Scintec Sodar- RASS as a so-called bi-static, acoustical pulse modulated system. This means that the acoustic signal is a frequency-modulated pulse and that the electromagnetic signal is transmitted continuously during RASS operation. The properties of the pulse modulation are configurable in the sodar operation software APRun (for details, see the Software Manual).

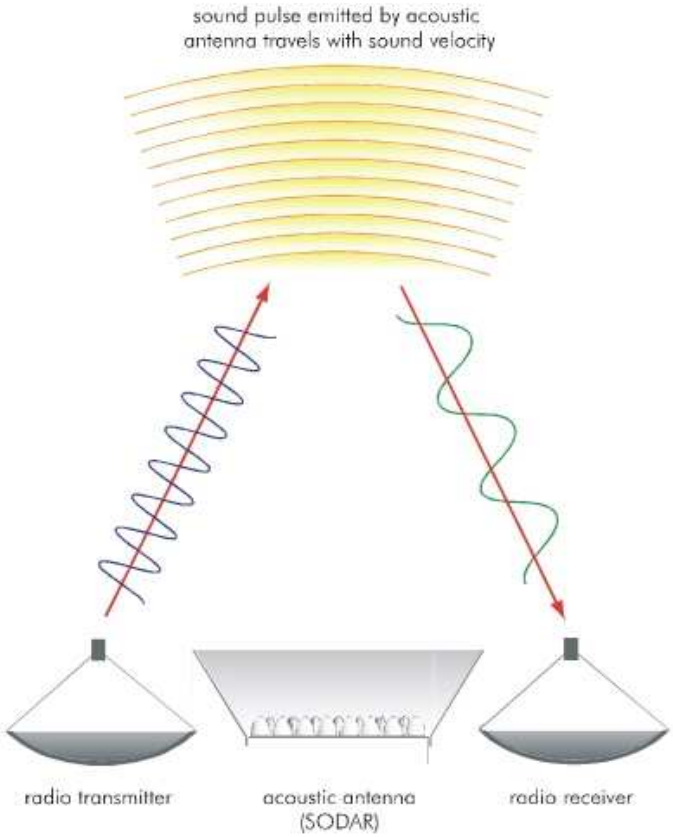

Figure 2: RASS working principle

3.1 Velocity of Sound

RASS signals register at the receiver if the wavelength λ_a of the sound waves and the wave length λ of the electromagnetic waves fulfil a Bragg condition, i.e.,

$$\lambda = 2\lambda_a \qquad \textbf{(42)}$$

Only in this case the reflections from matching region(s) of the emitted acoustic wave train add up coherently and are strong enough to be detectable. Since we scatter at moving density perturbations, the received electromagnetic waves are Doppler shifted in frequency by the amount Δf with respect to the emitted electromagnetic signal at f_0,

$$\Delta f = -2\frac{c_a + w}{c} f_0 \qquad \textbf{(43)}$$

For known vertical wind velocity w, speed of the electromagnetic waves in air c, and emitted electromagnetic frequency f_0, we can deduce the sound velocity c_a from a measurement of this Doppler shift. The height information is obtained by use of Eq. (13), which, introduced into (14), yields

$$\Delta f = -f_a - 2\frac{w}{c} f_0 \qquad \textbf{(44)}$$

where f_a is the acoustic frequency of that part of the wave train which fulfils the Brag condition (13) at the moment of reception of the electromagnetic signal. As we have control over the frequencies of the emitted acoustic signal, we can deduce the current position of the wave train element in question. We now have knowledge of the speed of sound as a function of vertical position above the Sodar/RASS.

3.2 Temperature

The temperature profile is derived by making use of the known square-root relationship between temperature T (in Kelvin), mixing ratio r (g/g) and speed of sound c_a (in m/s):

$$c_a = 20.067\sqrt{T(1+0.61r)} \qquad \textbf{(45)}$$

The quantity under the square root is known as the virtual temperature

$$T_v = T(1+0.61r) \qquad \textbf{(46)}$$

which is thus directly accessible by a RASS measurement. If the specific humidity q is known as a function of height or, assuming perfect mixing, by measurement on the ground, then the temperature T can be found as a function of height.

Please note that the acoustic frequencies leading to RASS signals depend on the temperature and on the frequency of the electromagnetic signal. APRun will attempt to automatically track the temperature with the acoustic frequencies chosen if the appropriate options are selected. If the electromagnetic frequency is 1290 MHz[*], then the acoustic frequencies are in the vicinity of 3 kHz.

If measurements for q are not available then it is possible to substitute the relative humidity h and the air pressure p, which determine q by

$$q = 0.622h\frac{e^*}{p - 0.378e^*} \qquad \textbf{(47)}$$

where e^* is the saturation vapour pressure. Above liquid containing surfaces as wet soil or water surfaces, e^* takes the approximate value (in Pa) (Bolton, 1980)

[*] 1290 MHz is the standard frequency. The RASS hardware can be equipped for a customer-specific frequency.

$$e^* = 6.112 \exp\left(\frac{17.67(T - 273.15)}{T - 29.65}\right) \quad \textbf{(48)}$$

Finally it should be noted that the specific humidity is related to the mixing ratio *r* by

$$q = r\frac{1}{1+r} \quad \textbf{(49)}$$

so that $q \approx r$ for small *q*.

4 windRASS Theory

The windRASS extension is an enhanced type of RASS extension, which exists of four pairs of dual-bar antennas located North, East, South and West of the sodar antenna. Two pairs emit the radio signal and the other two receive the backscattered radio signal. As the parabolic RASS antenna emits only one beam in the vertical direction, the dual-bar windRASS antenna emits five main beams (see Figure 3) simultaneous.

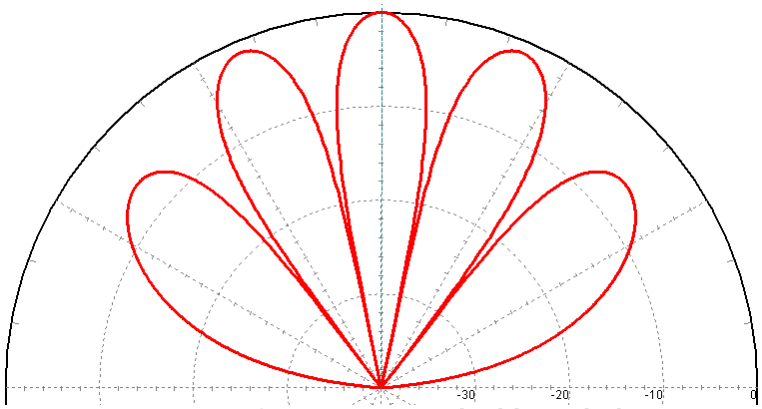

Figure 3: Beam pattern for a 1290 MHz dual-bar windRASS antenna

Within one measurement cycle, the acoustic signal is transmitted in five alternating directions; one vertical beam and four horizontal beams. Only the radio signal what is transmitted in the same direction is reflected at the acoustic signal and received at the windRASS antenna (see Figure 4). This permits to measure not only profiles of air temperature like the RASS extension but also profiles of horizontal wind using Radio Acoustic Sounding techniques.

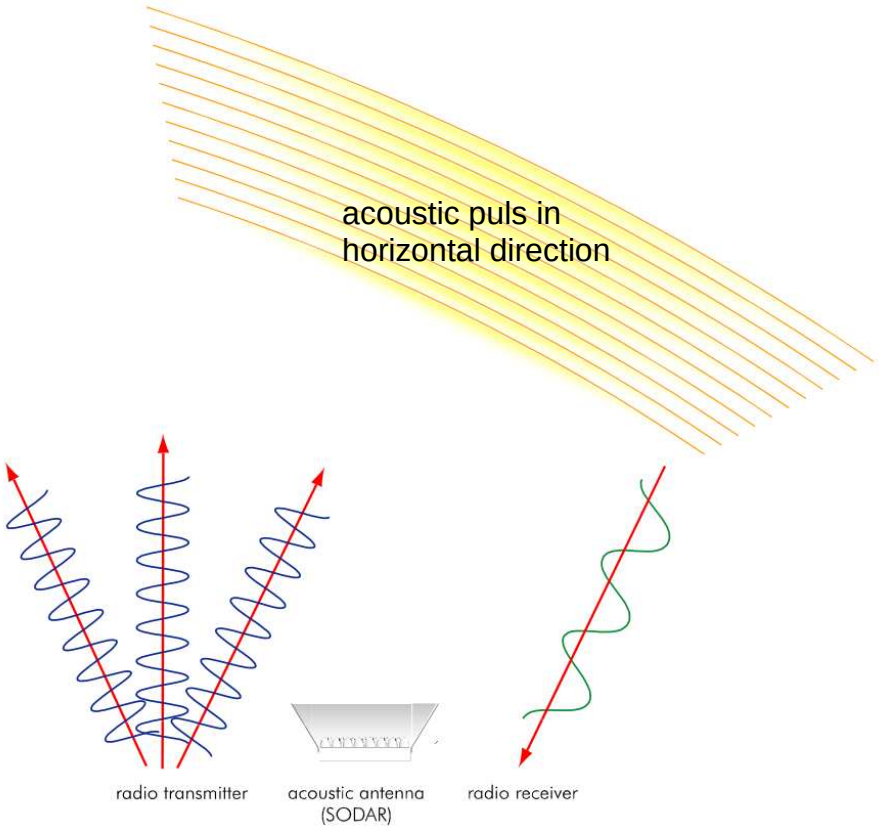

Figure 4: windRASS working principle

Compared to plain sodar wind measurements, Radio Acoustic Sounding employs some important advantages. It is insensitive to most site properties that limit plain sodar operation:

- The windRASS is insensitive to environmental acoustic noise.
- The windRASS is insensitive to ground clutter distortions.
- The windRASS operates under harshest environmental conditions.
- The windRASS allows for shorter averaging periods.

4.1 Horizontal Wind

The received electromagnetic waves from the vertical beam is Doppler shifted according to Eq. 43. The acoustic wave moves with the speed of sound and the mean vertical wind. As the vertical wind is very small compared to the speed of sound, the first is assumed zero.

The received electromagnetic waves from the horizontal beams are Doppler shifted in frequency by the amount Δf with respect to the emitted electromagnetic signal at f_0,

$$\Delta f = -2\frac{c_a + u_r}{c_l} f_0 \tag{50}$$

For known speed of sound c_a, speed of the electromagnetic waves in air c_l, and emitted electromagnetic frequency f_0, we can deduce the wind speed in beam direction u_r from a measurement of this Doppler shift.

When 4 directions with the tilted angles θ_E, θ_N, θ_W, θ_S are used with the frequencies f_E, f_N, f_W, f_S respectively, and we assume again that the horizontal wind is equal in each beam at the respective layers, then we can average over the Doppler shift at opposite beams. If $\theta_E = -\theta_W$ and $\theta_N = -\theta_S$, then the contributions of the vertical wind vanish. The wind speed in beam direction is calculated from the two opposite beams:

$$u_r = -\frac{1}{2}\left[\left(\frac{\Delta f_E}{2 f_E} c_l - c_a\right) + \left(\frac{\Delta f_W}{2 f_W} c_l - c_a\right)\right] \tag{51}$$

$$v_r = -\frac{1}{2}\left[\left(\frac{\Delta f_N}{2 f_N} c_l - c_a\right) + \left(\frac{\Delta f_S}{2 f_S} c_l - c_a\right)\right] \tag{52}$$

Using the beam angle θ the horizontal wind components, u and v, are calculated:

$$u = \frac{u_r}{\sin(\theta)} \tag{53}$$

$$v = \frac{v_r}{\sin(\theta)} \tag{54}$$

The horizontal wind direction is calculated according to Eq. 20.

5 Atmospheric Effects on System Performance

The range performance of all sodars depends on atmospheric conditions, which can change dramatically and rapidly. An inexperienced operator, when confronted with a reduced height range or large “holes” in the data, may assume that the sodar is not working properly, when in fact the sodar is working correctly, but the atmospheric conditions have changed. The conditions that most affect sodar and/or RASS performance are: temperature, humidity, turbulence and high winds.

5.1 Temperature and Humidity

Acoustic attenuation varies as a function of temperature, humidity, and pressure. Cold dry air exhibits highest attenuation, which can exceed -40 dB per kilometer. Very moist or warm air propagates acoustic signals better, resulting in improved range for the sodar measurements.

5.2 Turbulence

The amount of turbulence in the atmosphere affects the range performance of the sodar. The more turbulence there is in the atmosphere, particularly turbulence with a scale of one-half the sodar wavelength, the better the sodar works. The sodar data has a low signal-to-noise ratio when the air is stable with laminar airflows, a condition commonly found at night. This is because there is little thermally created turbulence available to reflect the sodar’s signals. Convective conditions can produce strong turbulence and correspondingly good sodar data, commonly found at daytime.

Turbulence is also beneficial to RASS operation. Turbulence helps distribute the acoustic wave front, helping increase the range in the presence of winds.

5.3 High Wind Speeds

High winds can adversely affect the sodar and the RASS measurement. High winds can cause clutter signals from objects such as trees and power lines slightly moving with the wind. This increased ground clutter can create incorrect sodar wind measurements. High winds may also reduce the range of measurement of RASS by displacing the acoustic signal away from the radar beam.

5.4 Ground Clutter

Higher obstacles like buildings, trees or hills within the sensing range of the sodar may reflect sound pulses and disturb the measurements. This effect is called "ground clutter" or “fixed echos”. With fixed echoes, typically a reduction of the measured wind velocities is observed due to the (usually) zero velocity of the reflecting surfaces at the respective height or distance. In addition, increased backscatter values typically result. The disturbances most often affect the quality of data in the lower measurement levels. Ground clutter is the most common source of problems with sodar measurements in general.

6 REFERENCES

Bradley, S., 2008: *Atmospheric acoustic remote sensing*, CRC Press

Bolton, D: 1980, *The Computation of Equivalent Potential Temperature*, Monthly Weather Review, Volume 108, p 1046-1053

EPA: 2000, *Meteorological Monitoring Guidance for Regulatory Modeling Applications*, U.S. Environmental Protection Agency, EPA-454/R-99-005

Kouznetsov, R. D.: 2000: *On the use of Kolmogorov–Prandtl semiempirical theory to estimate turbulence characteristics by sodar*. Proc. 10th Int. Symp. on Acoustic Remote Sensing, Auckland, New Zealand, ISARS, 142–144.

Kramar, V. F. and R. D. Kouznetsov: 2001: *A New Concept for Estimation of Turbulent Parameter Profiles in the ABL Using Sodar Data*, J. Atmos. Oceanic Technol. Volume 19, p 1216-1224

Melas, D. et al.: 2000, *Estimation of Meteorological Parameters for Air Quality Management: Coupling of Sodar Data with Simple Numerical Models*, Journal of Applied Meteorology, Volume 39, p. 509-515